Received 9 May 2024; Accepted 20 August 2024
https://doi.org/10.48612/letters/2024-3-262-268
https://elibrary.ru/mzbfhi

Debye temperature, electron-phonon coupling constant, and three-dome shape of crystalline strain as a function of pressure in highly compressed $La_3Ni_2O_{7-\delta}$

E. F. Talantsev†, V. V. Chistyakov

†evgeny.talantsev@imp.uran.ru

M. N. Miheev Institute of Metal Physics, Ural Branch, Russian Academy of Sciences, Ekaterinburg, 620108, Russia

Abstract: Besides ongoing studies of phase structural transitions, pairing mechanism, and physical properties of recently discovered highly compressed high-temperature superconductor $La_3Ni_2O_{7-\delta}$, here we explored a possibility for the electron-phonon pairing mechanism as an origin of the superconducting state and determined the microcrystalline strain, ε, in high-pressure *Fmmm*-phase, and low-pressure *Amam*-phase of this nickelate. To do this, we analysed temperature dependent resistance and extracted pressure dependent Debye temperature, Θ_D (P), in $La_3Ni_2O_{7-\delta}$ with an approximate value of $\Theta_D(25\ \text{GPa}) = 550$ K. From this we established that the $La_3Ni_2O_{7-\delta}$ is strong-coupled superconductor with the electron-phonon coupling constant $\lambda_{e\text{-}ph}(P = 22.4\ \text{GPa}) = 1.75$. This value is close to $\lambda_{e\text{-}ph} = 1.70$ of ambient pressure superconductors Nb_3R (R = Sn, Al). To address ongoing discussion that the lattice strain can be the origin for the emergence of high-temperature superconductivity in the $La_3Ni_2O_{7-\delta}$, we determined the microcrystalline strain, $0.011 \le \varepsilon(P)$, in the high-pressure *Fmmm*-phase, and $\varepsilon(P) < 0.011$ of low-pressure *Amam*-phase. Our analysis showed that ε(*P*) has three-dome shape in the pressure range of 1.6 GPa ≤ *P* ≤ 41.2 GPa. One of these two ε(*P*) deeps at *P* = 15 GPa coincides with the pressure at which the *Amam* into the *Fmmm* phase transition occurs. Based on our analysis, we proposed probable condition to observe the zero-resistance state in $La_3Ni_2O_{7-\delta}$.

Keywords: superconducting nickelates, high-pressure superconductivity, Debye temperature

Acknowledgements: *The authors thank financial support provided by the Ministry of Science and Higher Education of Russia (theme "Pressure" No. 122021000032-5, and theme "Spin" No. 122021000036-3).*

1. Introduction

Experimental discovery of superconductivity with a transition temperature above 200 K in highly compressed sulphur hydride by Drozdov et al [1] manifested a new era in superconductivity. In the following years from this pivotal discovery [1], dozens of superconducting hydride phases have been discovered [2 – 4] and several fundamental effects have been recorded [5 – 7]. Fascinating feature of this research field is that experimental and first-principles calculations (FPC) quests in exploring the ultimate upper limit in superconductivity are in close collaboration [8].

High-temperature superconductivity in nickelates was predicted by Anisimov et al [9], and experimental discovery of the superconductivity with transition temperature $T_{c,zero} \approx 15$ K in $Nd_{0.80}Sr_{0.20}NiO_2$ thin films were reported by Li et al[10]. Recently, the family of highly pressurized superconductors was extended by another nickelate phase [11–14], $La_3Ni_2O_7$, which surpasses other nickelate phases with the highest T_c. Phase structural transition, pairing mechanism, superconducting gap symmetry and other properties/parameters of the $La_3Ni_2O_7$ are under ongoing theoretical and experimental investigations.

We need to mention that that there are some current experimental and theoretical challenges to explain the superconductivity in the nickelates. For instance, doped $RNiO_2$ (R = La, Pr, Nd) exhibits superconductivity with $T_{c,zero} \ge 1.9$ K, but only in thin films of several nanometers thick. Bulk samples do not exhibit any sign of superconductivity down to $T_{c,onset} < 1.9$ K [15]. However, researchers very rarely mention this problem in the majority of theoretical and experimental studies, leading to a lack of understanding regarding the primary mechanism for the superconductivity in the nickelates.

Another example is the superconductivity in atomically thin quintuple-layer square-planar nickelate superlattice[16], for which only a single ρ(*T*) dataset has been revealed. In Fig. 1 we showed a low-temperature part of this ρ(*T*) dataset.

Simple examination of this experimental data shows that the $Nd_6Ni_5O_{12}$ exhibits the lowest measured resistance:

$$\rho(T = 53\ \text{mK}) = 6.3\ \mu\Omega \times \text{cm} \quad (1)$$

which is higher than the resistivity of practically all pure metals at room temperature [17]:

$$\rho(T = 300\ \text{K}) < 6.3\ \mu\Omega \times \text{cm} \quad (2)$$

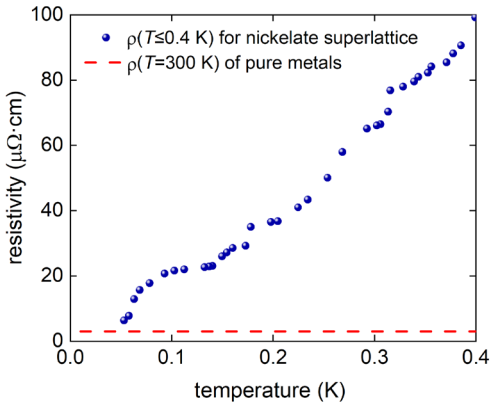

Fig. 1. (Color online) Temperature dependent resistivity, ρ(T≤0.4 K), reported in quintuple-layer square-planar nickelate $Nd_6Ni_5O_{12}$ (raw data reported by Pan et al [16]). Red dash line of ρ(T = 300 K) = 3 μΩcm is typical value for pure metals (see, for instance, Ref. [17]).

In addition, Pan et al. [16] did not report the uncertainty level of the measurements, thus, we cannot agree that these authors observed the superconducting state in quintuple-layer square-planar nickelate $Nd_6Ni_5O_{12}$ [16].

Two recent studies[12,18] have reported zero-resistance in the $La_3Ni_2O_7$. However, it is clearly stated in Ref. [18] that not all highly compressed $La_3Ni_2O_{7-\delta}$ samples exhibit zero-resistance transition. In addition, Zhou et al [18] reported the temperature dependent AC susceptibility data, from which it was estimated the presence of the superconducting phase at the volume level of 1% in the sample compressed at P ≥ 20 GPa. This result demonstrates that there is a quest to find an intriguing unknown parameter, which determines the appearance of the zero-resistance phase in highly compressed $La_3Ni_2O_{7-\delta}$.

Here, we contributed to the exploration and focused on a detailed analysis of available experimental data measured in highly compressed $La_3Ni_2O_{7-\delta}$ single crystals. While the majority of theoretical groups (but not all [19, 20]) explore hypotheses for unconventional mechanisms of pairing in the $La_3Ni_2O_7$, we investigated a possibility for the electron-phonon pairing mechanism.

To do this, we extracted:

1. pressure dependent Debye temperature, $\Theta_D(P)$; and based on that, we determined:

2. the electron-phonon coupling constant, $\lambda_{e\text{-}ph}$, for one sample exhibited the zero-resistance state.

In addition, we estimated:

3. the crystal lattice strain, ε(P), in the $La_3Ni_2O_{7-\delta}$ at nanoscale level.

Primary idea to determine the lattice strain, ε, was initiated by recent FPC result by Sanna et al[21] who reported that the record-high T_c in titanium[22,23] can be explained within electron-phonon phenomenology, if an assumption about the presence of the vacancies in the crystal lattice can be made. In addition, Liu et al [24] performed the FPC studies and concluded that the presence of the apical-oxygen vacancies should dramatically suppress superconducting transition temperature in $La_3Ni_2O_{7-\delta}$. On the other hand, vacancies are well-known structural imperfections which impact the superconducting state in cuprates [25,26] and iron-based superconductors [27]. It should be also noted that there is some experimental evidence that the lattice strain influences the superconducting transition in doped $RNiO_2$ (R = La, Pr, Nd) films[28].

The clearest expressions that the FPC studies should change its primary research object from the ideal defect-free crystal lattices to lattices with defects and strain has been reported by Cucciari et al [29].

While there are no experimental techniques which can be used for direct observation of the vacancies or other defects for samples in DAC, here we utilized the Williamson-Hall (WH) analysis [30] of the XRD data to extract the lattice strain, ε, in $La_3Ni_2O_{7-\delta}$. Advanced WH analysis [31–33] can be used to extract several microstructural parameters. However, here we used classical WH approach [30] to extract the lattice strain, ε, only, because of the high anisotropic crystallographic nature of the $La_3Ni_2O_7$ lattice, unknown Burgers vectors, b, and other unknown structural parameters are required for the advanced analysis.

It should be mentioned that two research groups [28,34] reported that the lattice strain impacts the superconducting and magnetic properties of the $RNiO_2$ thin films. In addition, Cui et al [35] reported that tensile strain stabilizes high-order Ruddlesden–Popper (RP) nickelates ($La_{n+1}Ni_nO_{3n+1}$) nickelates, whereas compressive strain favours to the low-order $La_3Ni_2O_7$ (which is $La_{n+1}Ni_nO_{3n+1}$ at n = 2). More recently, Oppliger et al [36] discovered a new phase of the infinite layer nickelate exhibited giant unit cell. It should be also noted, that microcrystalline strain/phase transitions in superconductors can be induced not only by high-pressure, but also by ionizing irradiation[37,38].

All of above facts are confirmations that the evolution of the ε(P) is important parameter which needs to be determine in any high-pressure superconductor.

2. Experimental data sources

In this study, we analysed experimental datasets reported by Sun et al [11]. We also analysed the $R(T)$ curve reported by the same research group in Fig. S9 in Ref. [39] and determined the $\lambda_{e\text{-}ph}(P)$ for the sample with a zero-resistance state. Utilized models and mathematical routine for the analysis described within each section. All fits performed by our own codes created in the Origin software. We used one of the standard data weighting methods, which is the method where the weight is proportional to the 1/standard deviation ratio (this method named "Instrumental" in the Origin software).

3. Results and discussion

Standard technique to determine the Debye temperature, Θ_D, is the fit of the specific heat measurements to Debye model. However, this technique cannot be used in studies of highly compressed conductors because of negligible sample thermal mass in comparison with the DAC mass. However, the fit of $R(T)$ data using the saturated resistance model [40,41] allows for the deduction of Θ_D as a free-fitting parameter:

$$R(T) = \frac{1}{\frac{1}{R_{sat}} + \frac{1}{R_0 + A \times \left(\frac{T}{\Theta_D}\right)^5 \times \int_0^{\frac{\Theta_D}{T}} \frac{x^5}{\left(e^x - 1\right)\left(1 - e^{-x}\right)} dx}}, \quad (1)$$

where R_{sat}, R_0, Θ_D and A are free-fitting parameters.

In Fig. 2, we showed the curves and data fits to Eq. (1) for samples Run 1 [11]. In Fig. S1 (Supplementary material), Fig. S2, and Fig. S3, we showed the curves and data fits to Eq. (1) for samples Run 2, 3, 4 [11], respectively. *R*-square coefficient of determination (*COD*) for each fit is given in each figure caption.

In Fig. 3 a we summarized all deduced $\Theta_D(P)$ values for all samples for which $R(T,P)$ datasets reported in Ref. [11].

One can see that in the pressure range where the high-pressure *Fmmm* phase exists, the Debye temperature is more or less constant with the approximate value of $\Theta_D = 550$ K.

Considering that Sun et al [11] reported that $T_{c,onset}(P)$ is practically unchanged for pure *Fmmm* phase, a hypothesis about the electron-phonon mediated superconductivity in $La_3Ni_2O_{7-\delta}$ remains its validity, until more experimental data will be available.

From deduced Θ_D and known T_c, the electron-phonon coupling constant, $\lambda_{e\text{-}ph}$, can be determined as the root of advanced McMillan equation [42]:

$$T_c = \left(\frac{1}{1.45}\right) \times \Theta_D \times e^{-\left(\frac{1.04\left(1+\lambda_{e-ph}\right)}{\lambda_{e-ph}-\mu^*\left(1+0.62\lambda_{e-ph}\right)}\right)} \times f_1 \times f_2^*, \quad (2)$$

where

$$f_1 = \left(1+\left(\frac{\lambda_{e-ph}}{2.46\left(1+3.8\mu^*\right)}\right)^{3/2}\right)^{1/3}, \quad (3)$$

$$f_2^* = 1+\left(0.0241-0.0735\times\mu^*\right)\times\lambda_{e-ph}^2, \quad (4)$$

where μ^* is the Coulomb pseudopotential. In this work we assumed that $\mu^* = 0.13$, which is a typical value for highly compressed electron-phonon mediated superconductors [8].

Considering all issues mentioned in the Introduction regarding the zero-resistance problem in nickelates, here we analysed the $R(T, P = 22.4$ GPa) measured in single crystal $La_3Ni_2O_{7-\delta}$ [39], and in which the resistance reduces to undistinguishable, from measurement system noise, level. To extract Θ_D and T_c, we utilized full $R(T)$ curve fitting[43]:

$$R(T) = \frac{1}{\frac{\theta\left(T_c^{onset}-T\right)}{R_0\left(T_c^{onset}\right)}+\theta\left(T-T_c^{onset}\right)\times\left(\frac{1}{R_{sat}}+\frac{1}{R_0+A\times\left(\frac{T}{\Theta_D}\right)^5\times\int_0^{\frac{\Theta_D}{T}}\frac{x^5}{\left(e^x-1\right)\left(1-e^{-x}\right)}\cdot dx}\right)}, \quad (5)$$

where $\theta(x)$ is the Heaviside step function, $I_0(x)$ is the zero-order modified Bessel function of the first kind, $R_0(T_c^{onset})$, T_c^{onset}, F, R_{sat}, R_0, Θ_D, and A are free-fitting parameters. We defined the transition temperature by the criterion:

$$\left.\frac{R(T)}{R\left(T_{c,onset}\right)}\right|_{T_{c,0.05}} = 0.05. \quad (6)$$

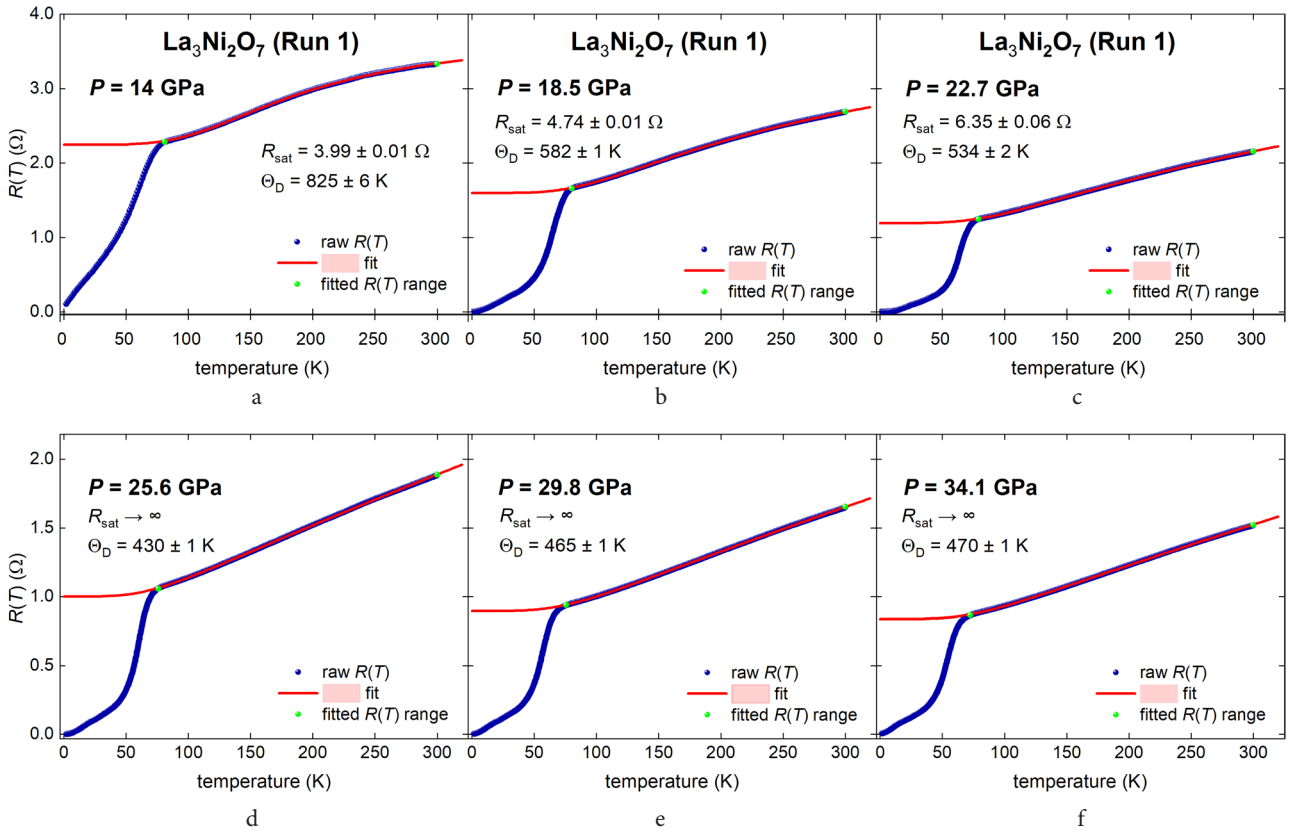

Fig. 2. (Color online) Temperature dependent resistance, $R(T,P)$, measured in compressed single crystal $La_3Ni_2O_7$ (Run 1) and data fits to Eq. (1). Raw data reported by Sun et al [11]. Green balls indicate the bounds for which $R(T)$ data was used for the fit to Eq. (1). Fit quality for all panels is better or equal to 0.9999. 95% confidence bands are shown by pink areas. $P = 14$ GPa (a); $P = 18.5$ GPa (b); $P = 22.7$ GPa (c); $P = 25.6$ GPa (d); $P = 14$ GPa (e); $P = 18.5$ GPa (f).

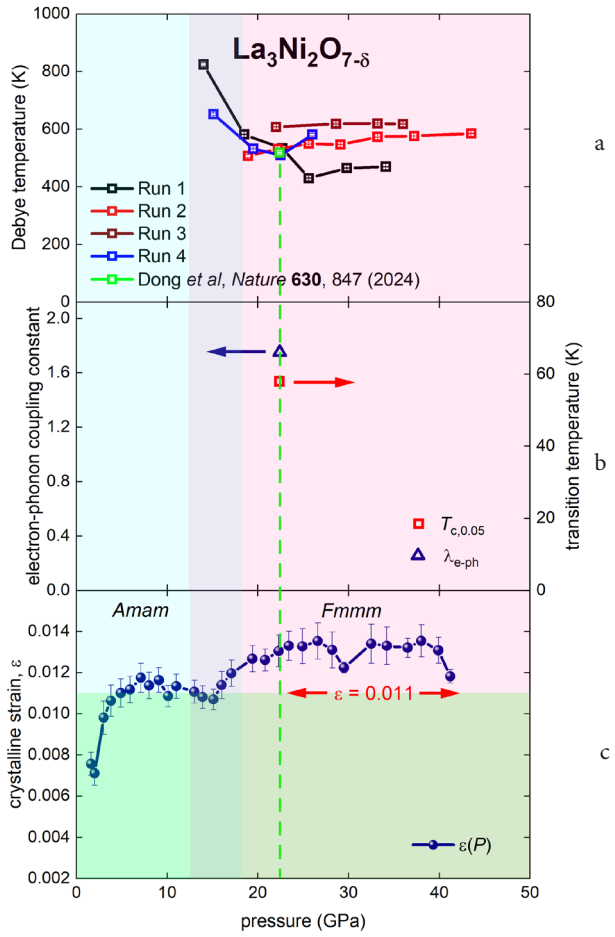

Fig. 3. (Color online) Evolution of the Debye temperature, $\Theta_D(P)$ on applied pressure (a); calculated electron-phonon coupling constant, $\lambda_{e\text{-}ph}$ (P = 22.4 GPa), and transition temperature defined by $T_{c,\,0.05}$(P = 22.4 GPa) criterion (b); and crystalline strain, $\varepsilon(P)$, in single crystal $La_3Ni_2O_{7-\delta}$ (c). Phase boundaries for the *Amma* and *Fmmm* phases are shown by magenta and cyan areas based on the estimated values reported by Sun et al [11].

The fit is shown in Fig. 4. It should be stressed that derived Θ_D (22.4 GPa) = 518 ± 4 K is practically the same for four of five analysed $R(T)$ datasets showed in Fig. 3.

Derived $T_{c,0.05}$ = 58.0 ± 0.1 K and $\lambda_{e\text{-}ph}$ = 1.75. Deduced $\lambda_{e\text{-}ph}$ shows, that if the high-temperature superconducting state in $La_3Ni_2O_{7-\delta}$ originates from the electron-phonon interaction, this requires the interaction strength at its upper limit, similar to the interaction strength exhibited in highly compressed hydrides [8, 44 – 47].

Derived $\lambda_{e\text{-}ph}$=1.75 value is close to $\lambda_{e\text{-}ph}$=1.70 of Nb_3Al and Nb_3Sn[48], and this value is significantly lower than the $\lambda_{e\text{-}ph}$ = 2.40 reported for ambient pressure oxide superconductor KOs_2O_6 [49].

XRD peaks [14] were approximated by Lorentz function:

$$I(2\theta) = I_{background} + \sum_{k=1}^{N} \frac{2 \times I_k}{\pi} \times \frac{\frac{2}{\pi}\beta_k}{4 \times \left(2\theta - 2\theta_{peak,k}\right)^2 + \left(\frac{2}{\pi}\beta\right)_k^2}, \quad (7)$$

where I_k is the peak area, $2\theta_{peak,k}$ is the peak position, β_k is peak integral breadth, and I_k, $2\theta_{peak,k}$, and β_k are-free fitting parameters. $I_{background}$ level was chosen manually in all fits. Details can be found elsewhere [50].

Derived peaks breadth, β(θ), and peaks diffraction angle, θ, were fitted to classical Williamson–Hall (WH) model [30] (where we assumed that the instrumental broadening, β_i, is negligible):

$$\beta(\theta, P) = \frac{0.9 \times \lambda_{X\text{-}ray}}{D(P) \times \cos(\theta)} + 4 \times \varepsilon(P) \times \tan(\theta), \quad (8)$$

where $\lambda_{X\text{-}ray}$ = 61.99 pm is the wavelength of used radiation in Ref. [11], and $D(P)$ is the mean size of coherent scattering regions at a given pressure P. As we mentioned above, in these fits, we used the weighting method of 1/standard deviation.

Performed fits showed that for all pressures, 1.6 GPa ≤ P ≤ 41.2 GPa, the size of coherent scattering regions, $D(P)$, is large and the uncertainty of the value exceeds the value itself by far. Thus, we fit data to the reduced equation:

$$\beta(\theta, P) = 4 \times \varepsilon(P) \times \tan(\theta). \quad (9)$$

We show some fits in Fig. S4, and we summarised results in Figs. 3 c, and 5, where one can see that the $\varepsilon(P)$ is raising reasonably steep at low applied pressure, up to P = 4.9 GPa.

We detected two deeps in the $\varepsilon(P)$ at P=15.1 GPa and 29.5 GPa (Figs. 3 c and 5). Our analysis showed

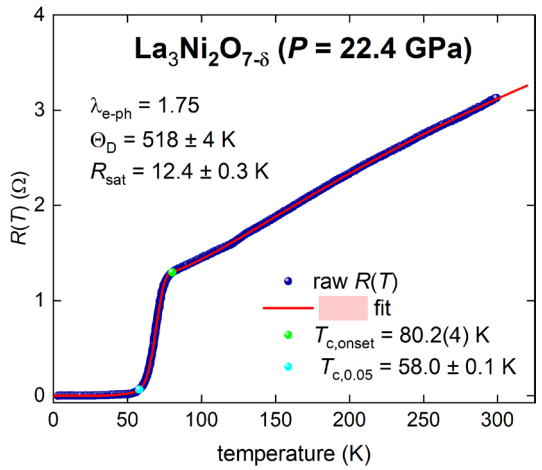

Fig. 4. (Color online) Temperature dependent resistance, $R(T,P$ = 22.4 GPa), in compressed single crystal $La_3Ni_2O_{7-\delta}$ and data fit to Eq. (5). Raw data reported by Dong et al [39] Fit quality is 0.99994.

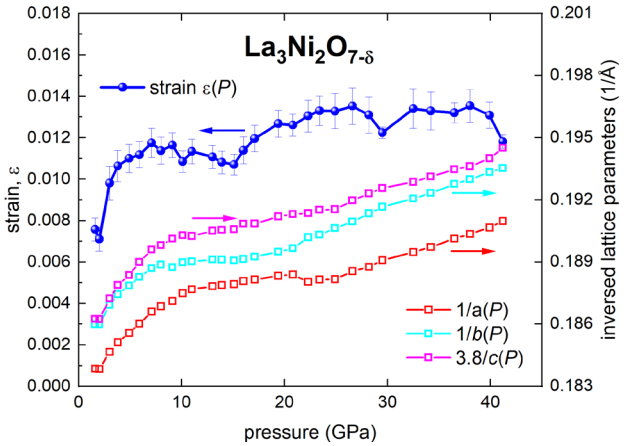

Fig. 5. (Color online) Crystalline strain, $\varepsilon(P)$, and inverse lattice constants $a(P)$, $b(P)$, and $c(P)$ dependence from applied pressure in highly compressed single crystal $La_3Ni_2O_{7-\delta}$. Raw data for $a(P)$, $b(P)$, and $c(P)$ reported by Sun et al [11].

that $\varepsilon(P)$ has three-dome shape in the pressure range of 1.6 GPa $\le P \le$ 41.2 GPa with peaks located at $P \cong 8, 25$, and 36 GPa (Figs. 3 c and 5).

The first deep at P=15.1 GPa coincides with the transition pressure from the *Amam* into the *Fmmm* phase, and perhaps it is direct structural evidence of the lattice relaxation at the structural transition.

However, the $\varepsilon(P)$ dependence does not exactly match the lattice constants dependences (see, $1/a(P)$, $1/b(P)$, and $1/c(P)$ in Fig. 5), especially at low- and high-P ranges. This difference, in particular, at low-P looks illogical.

However, we can explain the latter because of reducing the lattice volume by reducing the volume of each vacancy. This reduction can occur without significant changes in the lattice strain, because the vacancies density remains the same.

Perhaps, high vacancies density can be the origin for the observation/absence of the zero-resistance state in the $La_3Ni_2O_{7-\delta}$ [11]. Simple fact that there are no sharp simultaneous changes in $a(P)$, $b(P)$, $c(P)$, and $\varepsilon(P)$, except, perhaps, the change in curves slope at $P \approx 20$ GPa is an indication that the phase transition *Amam-Fmmm* is very wide.

We also need to stress that all XRD datasets (which we analysed) were collected at room temperature [11]. Obviously, that at the temperature range from T = 300 K down to T = 50 K some phase structural transition, or multiple transitions, can occur.

Another important revealed issue is that the level of the microcrystalline strain, $\varepsilon(P)$, in the *Amam*-phase of the $La_3Ni_2O_{7-\delta}$ samples is higher than the one measured in perfect undoped $YBa_2Cu_3O_{7-\delta}$ films [51, 52], $0.0039 \le \varepsilon_{YBCO\ film} \le 0.0078$. Thus, the *Fmmm*-phase exhibits significantly higher microcrystalline strain in comparison with undoped $YBa_2Cu_3O_{7-\delta}$. It would be interesting to determine the microcrystalline strain in recently discovered iron-based [53 – 56] and hydrogen-based superconductors [57 – 60] to build generic picture on the impact of microcrystalline stain on superconducting properties of high-temperature superconductors. First study of the crystalline strain at nanoscale level in hydrogen-based superconductor La_4H_{23} (with $T_{c,zero} \approx 70$ K) has performed recently [50]. This study [50] showed that the La_4H_{23} has a low level of strain $|\varepsilon(P)| \le 0.003$.

Based on all above, we should note that there is a need for low-temperature high-pressure XRD studies of $La_3Ni_2O_{7-\delta}$, which can be used for detailed analysis of the phase transition(s) and related structural/phase parameters.

4. Conclusions

Highly compressed $La_3Ni_2O_{7-\delta}$ is under intensive experimental and theoretical studies at the moment [11–14, 20, 35, 36, 39, 61, 62]. In this work, we analyzed experimental data and determined:

1. pressure dependent Debye temperature, $\Theta_D(P)$;
2. three-dome shape of the $\varepsilon(P)$ in the studied pressure range, where one deep of the $\varepsilon(P)$ coincides with the pressure at which the *Amam* into the *Fmmm* phase transition occurs; and
3. electron-phonon coupling constant, $\lambda_{e\text{-}ph}(P = 22.4\ \text{GPa}) = 1.75$;

in single crystal $La_3Ni_2O_{7-\delta}$.

Supplementary material: *The online version of this paper contains supplementary material (analysis for temperature dependent resistance data, and XRD data) freely available at the journal's web site https://lettersonmaterials.com.*

References

1. A. P. Drozdov, M. I. Eremets, I. A. Troyan, V. Ksenofontov, S. I. Shylin, Conventional superconductivity at 203 kelvin at high pressures in the sulfur hydride system, Nature 525 (2015) 73 – 76.
2. A. P. Drozdov, P. P. Kong, V. S. Minkov, S. P. Besedin, M. A. Kuzovnikov, S. Mozaffari, L. Balicas, F. F. Balakirev, D. E. Graf, V. B. Prakapenka, E. Greenberg, D. A. Knyazev, M. Tkacz, M. I. Eremets, Superconductivity at 250 K in lanthanum hydride under high pressures, Nature 569 (2019) 528 – 531.
3. M. Somayazulu, M. Ahart, A. K. Mishra, Z. M. Geballe, M. Baldini, Y. Meng, V. V. Struzhkin, R. J. Hemley, Evidence for Superconductivity above 260 K in Lanthanum Superhydride at Megabar Pressures, Phys. Rev. Lett. 122 (2019) 027001.
4. M. I. Eremets, The current status and future development of high-temperature conventional superconductivity, National Science Review 11 (2024) nwae047.
5. V. S. Minkov, S. L. Bud'ko, F. F. Balakirev, V. B. Prakapenka, S. Chariton, R. J. Husband, H. P. Liermann, M. I. Eremets, Magnetic field screening in hydrogen-rich high-temperature superconductors, Nat. Commun. 13 (2022) 3194.
6. V. S. Minkov, V. Ksenofontov, S. L. Bud'ko, E. F. Talantsev, M. I. Eremets, Magnetic flux trapping in hydrogen-rich high-temperature superconductors, Nat. Phys. 19 (2023) 1293 –1300.
7. P. Bhattacharyya, W. Chen, X. Huang, S. Chatterjee, B. Huang, B. Kobrin, Y. Lyu, T. J. Smart, M. Block, E. Wang, Z. Wang, W. Wu, S. Hsieh, H. Ma, S. Mandyam, B. Chen, E. Davis, Z. M. Geballe, C. Zu, V. Struzhkin, R. Jeanloz, J. E. Moore, T. Cui, G. Galli, B. I. Halperin, C. R. Laumann, N. Y. Yao, Imaging the Meissner effect in hydride superconductors using quantum sensors, Nature 627 (2024) 73 – 79.
8. L. Boeri, R. Hennig, P. Hirschfeld, G. Profeta, A. Sanna, E. Zurek, W. E. Pickett, M. Amsler, R. Dias, M. I. Eremets, C. Heil, R. J. Hemley, H. Liu, Y. Ma, C. Pierleoni, A. N. Kolmogorov, N. Rybin, D. Novoselov, V. Anisimov, A. R. Oganov, C. J. Pickard, T. Bi, R. Arita, I. Errea, C. Pellegrini, R. Requist, E. K. U. Gross, E. R. Margine, S. R. Xie, Y. Quan, A. Hire, L. Fanfarillo, G. R. Stewart, J. J. Hamlin, V. Stanev, R. S. Gonnelli, E. Piatti, D. Romanin, D. Daghero, R. Valenti, The 2021 room-temperature superconductivity roadmap, J. Phys.: Condens. Matter 34 (2022) 183002.
9. V. I. Anisimov, D. Bukhvalov, T. M. Rice, Electronic structure of possible nickelate analogs to the cuprates, Phys. Rev. B 59 (1999) 7901 – 7906.
10. D. Li, K. Lee, B. Y. Wang, M. Osada, S. Crossley, H. R. Lee, Y. Cui, Y. Hikita, H. Y. Hwang, Superconductivity in an infinite-layer nickelate, Nature 572 (2019) 624 – 627.
11. H. Sun, M. Huo, X. Hu, J. Li, Z. Liu, Y. Han, L. Tang,

Z. Mao, P. Yang, B. Wang, J. Cheng, D.-X. Yao, G.-M. Zhang, M. Wang, Signatures of superconductivity near 80 K in a nickelate under high pressure, Nature 621 (2023) 493 – 498.
12. X. Chen, J. Zhang, A. S. Thind, S. Sharma, H. LaBollita, G. Peterson, H. Zheng, D. P. Phelan, A. S. Botana, R. F. Klie, J. F. Mitchell, Polymorphism in the Ruddlesden–Popper Nickelate $La_3Ni_2O_7$: Discovery of a Hidden Phase with Distinctive Layer Stacking, J. Am. Chem. Soc. 146 (2024) 3640 – 3645.
13. Y. Zhang, D. Su, Y. Huang, Z. Shan, H. Sun, M. Huo, K. Ye, J. Zhang, Z. Yang, Y. Xu, Y. Su, R. Li, M. Smidman, M. Wang, L. Jiao, H. Yuan, High-temperature superconductivity with zero-resistance and strange metal behavior in $La_3Ni_2O_{7-\delta}$ (2024) arXiv: 2307.14819.
14. J. Hou, P. T. Yang, Z. Y. Liu, J. Y. Li, P. F. Shan, L. Ma, G. Wang, N. N. Wang, H. Z. Guo, J. P. Sun, Y. Uwatoko, M. Wang, G.-M. Zhang, B. S. Wang, J.-G. Cheng, Emergence of High-Temperature Superconducting Phase in Pressurized $La_3Ni_2O_7$ Crystals, Chinese Phys. Lett. 40 (2023) 117302.
15. Q. Li, C. He, J. Si, X. Zhu, Y. Zhang, H.-H. Wen, Absence of superconductivity in bulk $Nd_{1-x}Sr_xNiO_2$, Commun. Mater. 1 (2020) 16.
16. G. A. Pan, D. Ferenc Segedin, H. LaBollita, Q. Song, E. M. Nica, B. H. Goodge, A. T. Pierce, S. Doyle, S. Novakov, D. Córdova Carrizales, A. T. N'Diaye, P. Shafer, H. Paik, J. T. Heron, J. A. Mason, A. Yacoby, L. F. Kourkoutis, O. Erten, C. M. Brooks, A. S. Botana, J. A. Mundy, Superconductivity in a quintuple-layer square-planar nickelate, Nat. Mater. 21 (2022) 160 – 164.
17. R. A. Matula, Electrical resistivity of copper, gold, palladium, and silver, J. Phys. Chem. Ref. Data 8 (1979) 1147 – 1298.
18. Y. Zhou, J. Guo, S. Cai, H. Sun, P. Wang, J. Zhao, J. Han, X. Chen, Y. Chen, Q. Wu, Y. Ding, T. Xiang, H. Mao, L. Sun, Investigations of key issues on the reproducibility of high-Tc superconductivity emerging from compressed $La_3Ni_2O_7$, (2023) arXiv: 2311.12361.
19. A. A. C. Alvarez, S. Petit, L. Iglesias, M. Bibes, W. Prellier, J. Varignon, Charge ordering as the driving mechanism for superconductivity in rare-earth nickel oxides, Phys. Rev. Materials 8 (2024) 064801.
20. J. Zhan, Y. Gu, X. Wu, J. Hu, Cooperation between electron-phonon coupling and electronic interaction in bilayer nickelates $La_3Ni_2O_7$ (2024) arXiv: 2404.03638.
21. A. Sanna, C. Pellegrini, S. di Cataldo, G. Profeta, L. Boeri, A possible explanation for the high superconducting T_c in bcc Ti at high pressure, Phys. Rev. B 108 (2023) 214523.
22. C. Zhang, X. He, C. Liu, Z. Li, K. Lu, S. Zhang, S. Feng, X. Wang, Y. Peng, Y. Long, R. Yu, L. Wang, V. Prakapenka, S. Chariton, Q. Li, H. Liu, C. Chen, C. Jin, Record high T_c element superconductivity achieved in titanium, Nat. Commun. 13 (2022) 5411.
23. X. Liu, P. Jiang, Y. Wang, M. Li, N. Li, Q. Zhang, Y. Wang, Y.-L. Li, W. Yang, T_c up to 23.6 K and robust superconductivity in the transition metal δ-Ti phase at megabar pressure, Phys. Rev. B 105 (2022) 224511.
24. Y.-B. Liu, J.-W. Mei, F. Ye, W.-Q. Chen, F. Yang, $s^{\pm}$-Wave Pairing and the Destructive Role of Apical-Oxygen Deficiencies in $La_3Ni_2O_7$ under Pressure, Phys. Rev. Lett. 131 (2023) 236002.
25. J. D. Jorgensen, H. Shaked, D. G. Hinks, B. Dabrowski, B. W. Veal, A. P. Paulikas, L. J. Nowicki, G. W. Crabtree, W. K. Kwok, L. H. Nunez, H. Claus, Oxygen vacancy ordering and superconductivity in $YBa_2Cu_3O_{7-x}$, Physica C: Supercond. 153 –155 (1988) 578 – 581.
26. S. Kh. Gadzhimagomedov, D. K. Palchaev, Zh. Kh. Murlieva, M. Kh. Rabadanov, M. Yu. Presnyakov, E. V. Yastremsky, N. S. Shabanov, R. M. Emirov, A. E. Rabadanova, YBCO nanostructured ceramics: Relationship between doping level and temperature coefficient of electrical resistance, Journal of Physics and Chemistry of Solids 168 (2022) 110811.
27. V. Grinenko, K. Kikoin, S.-L. Drechsler, G. Fuchs, K. Nenkov, S. Wurmehl, F. Hammerath, G. Lang, H.-J. Grafe, B. Holzapfel, J. Van Den Brink, B. Büchner, L. Schultz, As vacancies, local moments, and Pauli limiting in $LaFeAs_{1-\delta}O_{0.9}F_{0.1}$ superconductors, Phys. Rev. B 84 (2011) 134516.
28. X. Ren, J. Li, W.-C. Chen, Q. Gao, J. J. Sanchez, J. Hales, H. Luo, F. Rodolakis, J. L. McChesney, T. Xiang, J. Hu, R. Comin, Y. Wang, X. Zhou, Z. Zhu, Possible strain-induced enhancement of the superconducting onset transition temperature in infinite-layer nickelates, Commun. Phys. 6 (2023) 341.
29. A. Cucciari, D. Naddeo, S. Di Cataldo, L. Boeri, NbTi: a nontrivial puzzle for the conventional theory of superconductivity (2024) arXiv: 2403.15196.
30. G. K. Williamson, W. H. Hall, X-ray line broadening from filed aluminium and wolfram, Acta Metallurgica 1 (1953) 22 – 31.
31. A. Borbély, The modified Williamson-Hall plot and dislocation density evaluation from diffraction peaks, Scr. Mater. 217 (2022) 114768.
32. T. Ungár, Microstructural parameters from X-ray diffraction peak broadening, Scr. Mater. 51 (2004) 777 – 781.
33. T. Ungár, A. Borbély, The effect of dislocation contrast on x-ray line broadening: A new approach to line profile analysis, Appl. Phys. Lett. 69 (1996) 3173 – 3175.
34. I. Biało, L. Martinelli, G. De Luca, P. Worm, A. Drewanowski, S. Jöhr, J. Choi, M. Garcia-Fernandez, S. Agrestini, K.-J. Zhou, K. Kummer, N.B. Brookes, L. Guo, A. Edgeton, C.B. Eom, J.M. Tomczak, K. Held, M. Gibert, Q. Wang, J. Chang, Strain-tuned incompatible magnetic exchange-interaction in La_2NiO_4, Communications Physics 7 (2024) 230.
35. T. Cui, S. Choi, T. Lin, C. Liu, G. Wang, N. Wang, S. Chen, H. Hong, D. Rong, Q. Wang, Q. Jin, J.-O. Wang, L. Gu, C. Ge, C. Wang, J.G. Cheng, Q. Zhang, L. Si, K. Jin, E.-J. Guo, Strain-mediated phase crossover in Ruddlesden–Popper nickelates, Communications Materials 5 (2024) 32.
36. J. Oppliger, J. Küspert, A.-C. Dippel, M. v. Zimmermann, O. Gutowski, X. Ren, X. J. Zhou, Z. Zhu, R. Frison, Q. Wang, L. Martinelli, I. Biało, J. Chang, Discovery of Giant Unit-Cell Super-Structure in the Infinite-Layer Nickelate $PrNiO_2$ (2024) arXiv: 2404.17795.
37. E. M. Ibragimova, A. A. Shodiev, S. Ahrorova, M. A. Mussaeva, N. E. Iskandarov, U. T. Kurbanov,

M. Yu. Tashmetov, Low-dimensional magnetic centers in HTSC YBCO film on steel-276 induced by gamma-quanta and electron beam, J. Magn. Magn. Mater. 595 (2024) 171617.
38. S. B. L. Chislett-McDonald, L. Bullock, A. Turner, F. Schoofs, Y. Dieudonne, A. Reilly, *In-situ* critical current measurements of REBCO coated conductors during gamma irradiation, Supercond. Sci. Technol. 36 (2023) 095019.
39. Z. Dong, M. Huo, J. Li, J. Li, P. Li, H. Sun, L. Gu, Y. Lu, M. Wang, Y. Wang, Z. Chen, Visualization of oxygen vacancies and self-doped ligand holes in $La_3Ni_2O_{7-\delta}$, Nature 630 (2024) 847–852.
40. H. Wiesmann, M. Gurvitch, H. Lutz, A. Ghosh, B. Schwarz, M. Strongin, P. B. Allen, J. W. Halley, Simple Model for Characterizing the Electrical Resistivity in A–15 Superconductors, Phys. Rev. Lett. 38 (1977) 782–785.
41. E. F. Talantsev, Quantifying interaction mechanism in infinite layer nickelate superconductors, J. Appl. Phys. 134 (2023) 113904.
42. E. F. Talantsev, Advanced McMillan's equation and its application for the analysis of highly-compressed superconductors, Supercond. Sci. Technol. 33 (2020) 094009.
43. E. F. Talantsev, K. Stolze, Resistive transition of hydrogen-rich superconductors, Supercond. Sci. Technol. 34 (2021) 064001.
44. I. Errea, M. Calandra, C. J. Pickard, J. Nelson, R. J. Needs, Y. Li, H. Liu, Y. Zhang, Y. Ma, F. Mauri, High-Pressure Hydrogen Sulfide from First Principles: A Strongly Anharmonic Phonon-Mediated Superconductor, Phys. Rev. Lett. 114 (2015) 157004.
45. I. Errea, F. Belli, L. Monacelli, A. Sanna, T. Koretsune, T. Tadano, R. Bianco, M. Calandra, R. Arita, F. Mauri, J. A. Flores-Livas, Quantum crystal structure in the 250-kelvin superconducting lanthanum hydride, Nature 578 (2020) 66–69.
46. I. Errea, M. Calandra, C. J. Pickard, J. R. Nelson, R. J. Needs, Y. Li, H. Liu, Y. Zhang, Y. Ma, F. Mauri, Quantum hydrogen-bond symmetrization in the superconducting hydrogen sulfide system, Nature 532 (2016) 81–84.
47. I. A. Troyan, D. V. Semenok, A. G. Kvashnin, A. V. Sadakov, O. A. Sobolevskiy, V. M. Pudalov, A. G. Ivanova, V. B. Prakapenka, E. Greenberg, A. G. Gavriliuk, I. S. Lyubutin, V. V. Struzhkin, A. Bergara, I. Errea, R. Bianco, M. Calandra, F. Mauri, L. Monacelli, R. Akashi, A. R. Oganov, Anomalous High-Temperature Superconductivity in YH_6, Advanced Materials 33 (2021) 2006832.
48. J. P. Carbotte, Properties of boson-exchange superconductors, Rev. Mod. Phys. 62 (1990) 1027–1157.
49. Z. Hiroi, S. Yonezawa, Y. Nagao, J. Yamaura, Extremely strong-coupling superconductivity and anomalous lattice properties in the β-pyrochlore oxide KOs_2O_6, Phys. Rev. B 76 (2007) 014523.
50. E. F. Talantsev, V. V. Chistyakov, The A-15-type superconducting hydride La_4H_{23}: a nanograined structure with low strain, strong electron-phonon interaction, and a moderate level of nonadiabaticity, Supercond. Sci. Technol. 37 (2024) 095016.
51. M. Z. Khan, Y. Zhao, X. Wu, M. Malmivirta, H. Huhtinen, P. Paturi, Improved interface growth and enhanced flux pinning in YBCO films deposited on an advanced IBAD – MgO based template, Physica C: Superconductivity and Its Applications 545 (2018) 50 – 57.
52. M. O. Rikel, V. A. Amelichev, A. V. Markelov, P. N. Degtyarenko, A. A. Adamenkov, A. A. Kamenev, Advances in XRD Characterization of 2G HTS Wire for Low-Temperature Magnet Applications, IEEE Trans. Appl. Supercond. 34 (2024) 1–5.
53. A. V. Sadakov, A. A. Gippius, A. T. Daniyarkhodzhaev, A. V. Muratov, A. V. Kliushnik, O. A. Sobolevskiy, V. A. Vlasenko, A. I. Shilov, K. S. Pervakov, Multiband Superconductivity in $KCa_2Fe_4As_4F_2$, JETP Lett. 119 (2024) 111–117.
54. T. Kuzmicheva, K. Pervakov, V. Vlasenko, A. Degtyarenko, S. Kuzmichev, Temperature Dependence of the Superconducting Order Parameter in Stoichiometric Alkali Metal-Based Pnictide $EuCsFe_4As_4$, J. Supercond. Nov. Magn. 37 (2024) 379 – 388.
55. S. Kuzmichev, A. Muratov, S. Gavrilkin, I. Morozov, A. Shilov, Y. Rakhmanov, A. Degtyarenko, T. Kuzmicheva, Superconducting gap structure of slightly overdoped $NaFe_{0.955}Co_{0.045}As$ pnictides: joint SnS-Andreev spectroscopy and specific heat study, Eur. Phys. J. Plus 139 (2024) 74.
56. M. S. Sidelnikov, A. V. Palnichenko, K. S. Pervakov, V. A. Vlasenko, I. I. Zverkova, L. S. Uspenskaya, V. M. Pudalov, L. Ya. Vinnikov, Direct Observation of Pinning of Abrikosov Vortices in a Specially Inhomogenious Crystal $EuRbFe_4As_4$, JETP Lett. 119 (2024) 523 – 528.
57. I. A. Troyan, D. V. Semenok, A. G. Ivanova, A. V. Sadakov, D. Zhou, A. G. Kvashnin, I. A. Kruglov, O. A. Sobolevskiy, M. V. Lyubutina, D. S. Perekalin, T. Helm, S. W. Tozer, M. Bykov, A. F. Goncharov, V. M. Pudalov, I. S. Lyubutin, Non-Fermi-Liquid Behavior of Superconducting SnH_4, Adv. Sci. 10 (2023) 2303622.
58. J. Guo, D. Semenok, G. Shutov, D. Zhou, S. Chen, Y. Wang, K. Zhang, X. Wu, S. Luther, T. Helm, X. Huang, T. Cui, Unusual metallic state in superconducting A15-type La_4H_{23}, National Science Review (2024) nwae149.
59. X. Song, X. Hao, X. Wei, X.-L. He, H. Liu, L. Ma, G. Liu, H. Wang, J. Niu, S. Wang, Y. Qi, Z. Liu, W. Hu, B. Xu, L. Wang, G. Gao, Y. Tian, Superconductivity above 105 K in Nonclathrate Ternary Lanthanum Borohydride below Megabar Pressure, J. Am. Chem. Soc. 146 (2024) 13797–13804.
60. S. Chen, Y. Wang, F. Bai, X. Wu, X. Wu, A. Pakhomova, J. Guo, X. Huang, T. Cui, Superior Superconducting Properties Realized in Quaternary La-Y-Ce Hydrides at Moderate Pressures, J. Am. Chem. Soc. 146 (2024) 14105 –14113.
61. D. A. Shilenko, I. V. Leonov, Correlated electronic structure, orbital-selective behavior, and magnetic correlations in double-layer $La_3Ni_2O_7$ under pressure, Phys. Rev. B 108 (2023) 125105.
62. E. F. Talantsev, Solving Mystery with the Meissner State in La3Ni2O7−Δ, (2024), Available at SSRN